06.4;13.1

Change of the loop directions on the high-frequency capacitance-voltage characteristics at a critical bias voltage, dielectric properties and memory effects in the $Sr_{0.6}Ba_{0.4}Nb_2O_6/SrTiO_3/Si(001)$ heterostructure

© A.V. Pavlenko

Southern Scientific Center, Russian Academy of Sciences, Rostov-on-Don, Russia
E-mail: Antvpr@mail.ru

Received June 14, 2023
Revised July 28, 2023
Accepted July 31, 2023

A c-oriented barium-strontium niobate film of composition $Sr_{0.6}Ba_{0.4}Nb_2O_6$ (SBN60) with a thickness of 600 nm was grown by high-frequency cathode sputtering on a Si(001) substrate with a preliminarily deposited $SrTiO_3$ (STO) sublayer. It is shown that the film belongs to the relaxor ferroelectrics. When analyzing the high-frequency capacitance-voltage characteristics of the SBN60/STO/Si(001) heterostructure at $U = 0-24$ V, a critical electric voltage (~ 10 V) was established, in the vicinity of which a change in the $C(U)$ loop direction was observed. It is shown that the reason of loop direction change may be due to an increase in the role of the built-in charge, which is formed at the film-substrate interface, as the amplitude U increases, simultaneously with ferroelectric polarization switching in the SBN60 film. The causes of the revealed regularities and their role in the study of memory effects in the SBN60/STO/Si(001) heterostructure are discussed.

Keywords: barium-strontium niobate (SBN), metal-ferroelectric-semiconductor structures, thin films.

DOI: 10.61011/TPL.2023.10.57047.19652

Heterostructures based on ferroelectric (FE) films deposited directly onto semiconductor (SC) substrates are of interest in the design of memory elements, pyroelectric radiation detectors, and microelectromechanical systems [1]. The search for FE materials with the optimum composition and process technology to be used in SC engineering has been ongoing for years; complex oxides of various structural families are being examined actively [1–3]. Barium-strontium niobates $Sr_xBa_{1-x}Nb_2O_6$ (SBN) with the structure of tetragonal tungsten bronze (TTB), which, in contrast to ferroelectrics with perovskite or layered perovskite structures, are uniaxial materials in the form of nanodimensional films, are regarded as promising FE materials. However, although SBN single crystals with $x = 0.61$ (congruent composition) and $x = 0.75$ are used efficiently in optoelectronics and photorefractive and nonlinear optics, questions regarding the mechanisms of emergence of ferroelectric polarization [4,5] and dielectric properties (specifically, relaxor properties) [6] still remain relevant. Only textured (polycrystalline) SBN samples were grown on single-crystal silicon substrates [7–9]. However, their texture may be adjusted with the use of interlayers [9], which is important due to the fact that the FE polarization in SBN is directed strictly along (001), and the corresponding anisotropy of properties emerges. It was found in preliminary studies that $SrTiO_3$ (STO) (high-k dielectric with $\varepsilon = 310$ and $E_g = 3.2$ eV, a promising insulator for integrated circuits [1]) may fit the role of such an interlayer produced under process conditions similar to those of SBN. Completely *c*-oriented SBN films may be fabricated with the use of this interlayer with a thickness upward of ~ 10 nm. Since the examination of SBN films is of fundamental and applied importance when performed in the vicinity of the congruent composition (this ensures high permittivity values (> 900), high electrooptic ($r_{13} = 45$ pm/V, $r_{33} = 250$ pm/V) and pyroelectric ($0.065\,\mu C \cdot cm^{-2} \cdot K^{-1}$) coefficients, and proximity to the region of a normal ferroelectric $\rightarrow$ relaxor ferroelectric transition), the aim of the present study is to establish the patterns of formation of dielectric properties and memory effects in *c*-oriented $Sr_{0.6}Ba_{0.4}Nb_2O_6$(SBN60)/ STO/Si(001) films.

The patterns of variation of properties of FE films in the indicated structures within wide ranges of temperature and electric field intensity and the specific features of the „ferroelectric field effect“ [2] are crucial for their operation. Note that data on the values of x corresponding to a conventional ferroelectric $\rightarrow$ relaxor ferroelectric transition in SBN films and on the contribution of deformation of a lattice cell and the structural perfection of objects to this transition are currently lacking. It occurs at $x \geqslant 0.53$ [10] in ceramic materials and at $x \geqslant 0.60$ [11] in crystals. Owing to a lack of systematic studies, it is relevant to determine the type of ferroelectrics to which SBN films belong, since approaches based on measurements of capacitor metal/ferroelectric/metal structures, which are hardly suitable due to the influence of an SC substrate, are used to examine macroscopic dielectric and FE properties of metal–ferroelectric–semiconductor (MFS) heterostructures. The analysis of high-frequency capacitance–voltage characteristics under various external influences is one of the methods providing data both on the properties of films and on the ferroelectric–semiconductor interaction. This method

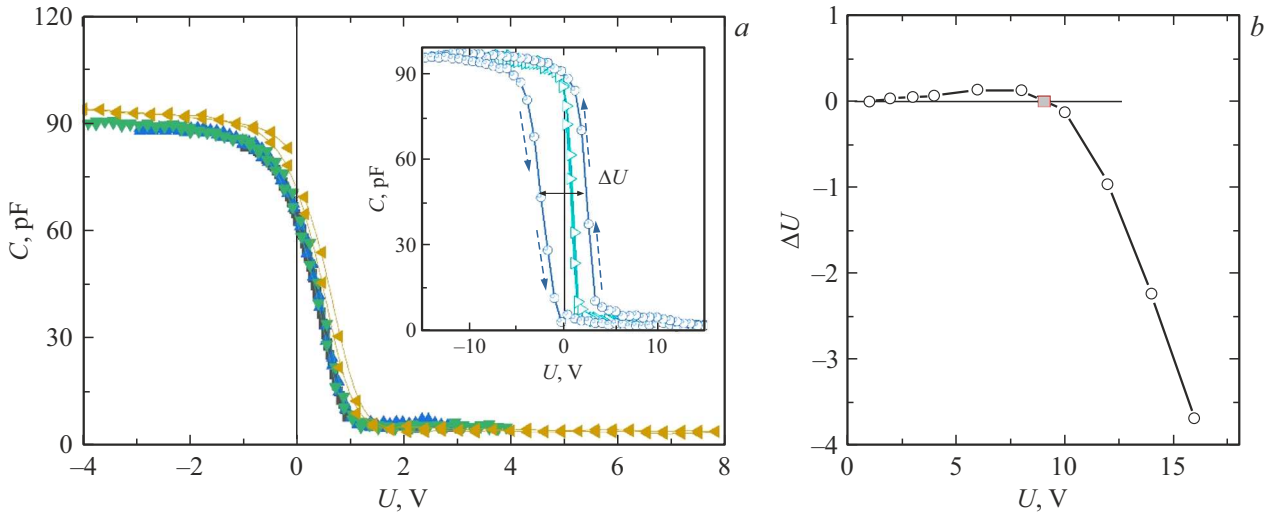

Figure 1. *a* — $C(U)$ dependences of the SBN60/STO/Si(001) heterostructure at room temperature and $f = 10$ kHz; *b* — dependence of width (ΔU) of dependence $C(U)$ on the amplitude of bias voltage. Dependences $C(U)$ at an amplitude of 10 V (circles) and 18 V (triangles) are shown in the inset.

relies on measurements of the dependence of capacitance C of a heterostructure at high frequencies (normally falling within the 10^4-10^6 Hz range, where the concentration of inverse electrons fails to follow the variation of alternating voltage applied to the structure) on the applied voltage. In the case of ideal MFS structures, parameters of the $C(U)$ dependence allow one to determine the permittivity value, the nature of polarization switching, the coercive field, and other characteristics of a ferroelectric [12]. However, significant deviations may emerge in real-world structures (see below).

SBN60 and STO films were deposited at different setups by radio-frequency cathode sputtering in the oxygen atmosphere. Si (001) (KDB-12, *p*-type, 12 Ω/cm, 360 μm in thickness, both sides polished) was used as a substrate. The thickness of SBN60 and STO was ~ 600 and ~ 10 nm, respectively (thicknesses were estimated based on the deposition time). According to the X-ray diffraction data, the SBN60 film was polycrystalline and *c*-oriented: axes [001] of lattice cells were oriented along the normal to the substrate surface (this is verified by the fact that only the (00*l*) reflections were present in the $\theta-2\theta$-scan pattern), and their axes [100] and [010] were oriented stochastically in the interface plane. Metal–ferroelectric–semiconductor structures were formed for dielectric measurements in the direction normal to the surface: Ag/Pd layers ~ 150 nm in thickness deposited by magnetron sputtering in the argon atmosphere at an Emitech SC7620 setup through a shadow mask with apertures 90–100 μm in diameter served as electrodes. Capacitance–voltage characteristics (CVCs) of objects at T varying from -100 to 200°C were measured with a TFAnalyzer2000 module and a Linkam THMS600 temperature control stage in order to examine the field effect in the MFS structure and the temperature dependence of relative permittivity ε of the SBN60 film. The sample capacitance was measured at frequencies of 10^4-10^5 Hz at $U = 40$ mV, and the frequency of the control triangular voltage with its amplitude varying from 0 to 24 V was 1 Hz.

Figure 1 presents the $C(U)$ dependences for the SBN60/STO/Si(001) heterostructure measured at a temperature of 20°C. All $C(U)$ dependences had the form of a high-frequency CVC for a metal–insulator–semiconductor (MIS) structure [13]. With the geometric positioning of layers taken into account, the sample capacitance in this case is $C = (1/C_{\mathrm{FE}} + 1/C_{\mathrm{Si}})^{-1}$, where C_{FE} is the capacitance of the ferroelectric film and C_{Si} is the capacitance of the silicon substrate. While quantity C_{FE} is related directly to ε and geometric dimensions of the FE film and its changes are induced by the dependence of ε on U, C_{Si} is a function of semiconductor characteristics: T and f (this dependence is presented, e.g., in [12], but it is insignificant in the present study, where the region with prevalent C_{FE} is analyzed). Let us examine the patterns of variation of capacitance C_{samp} of the entire sample in more detail. The minimum sample capacitance (Fig. 1) is $C_{\min} = 3.8$ pF, while the maximum is $C_{\max} = 96.5$ pF; prior to the impact of the field, the sample capacitance had an intermediate value $C_0 = 70$ pF. When positive voltage was applied to the film, the sample capacitance controlled by the capacitance of the depletion layer in the semiconductor, which separates the inversion layer from the quasineutral bulk, decreased from C_0 to $C_{\min}$. When negative voltage was applied, C_{samp} first increased to the level of $C_{\max}$, which is set by C_{FE}, and then decreased (this is not observed in MIS structures) due to a change in the FE film permittivity. As the voltage applied to the SBN60/STO/Si heterostructure increased, memory effects started to manifest themselves: CVCs became hysteretic, varying in type from a „polarization“ hysteresis to an „injection“ one, which has never been observed before in MFS structures based on barium-strontium niobates. The value of

ΔU (width of the $C(U)$ dependence at half height) increased from 0 to 0.4 V in weak fields (Fig. 1, *b*), but then ΔU decreased, reached zero (i.e., the $C(U)$ dependence became anhysteretic; see the inset in Fig. 1, *a*), and assumed negative values later on. The polarization-type hysteresis in CVCs of MFS structures is induced primarily by polarization switching in the ferroelectric material: $\Delta U = 2h_{\mathrm{SBN60}}E_C$ (E_C is the coercive field) [12], and the magnitude and direction of residual FE film polarization affect the state of the space charge region in the semiconductor substrate (enrichment, depletion, or inversion). The value of C_{samp} of the SBN60/STO/Si heterostructure at $U = 0$ V, which was observed after the application of $U < 10$ V, relaxed fairly rapidly (within 10 s) to the initial state, and „fatigue" was almost nonexistent through to 10^9 switching cycles n (Fig. 2). This is indicative of weakness of residual polarization in the studied SBN60 film (the same is true for single-crystal SBN50 films [14], which was estimated at 1.2 μC/cm^2, and stability of the material under multiple polarization switching. Note that a significant „fatigue," which was manifested, e.g., in C_{FE} reduction and a non-monotonic variation of ΔU, was observed in polycrystalline SBN60 films already after 10^6 switching cycles. It is known that $Sr_{1-x}Ba_xNb_2O_6$ solid solutions with $x > 0.5$ are relaxor ferroelectrics due to chaotic positioning of Sr and Ba cations at *A*1 (tetragonal) and *A*2 (pentagonal) sites of the TTB structure [6]. The following features of polarization processes typical of relaxor ferroelectrics and attributable to the domain structure specifics were observed numerous times in single crystals of these compositions: long relaxation times (up to several hours), irreproducibility of hysteresis loops, low-frequency E_C dispersion, etc. [15]. It can be seen from Fig. 3 that the studied SBN60 film is also a relaxor ferroelectric: dependences $\varepsilon(T)$are dome-shaped with frequency-dependent maxima in the vicinity of 40–45°C (the values of ε were calculated based on $C_{\max}$ in the $C(U)$ dependence measured at a fixed temperature). Burns temperature T_b, which corresponds to the temperature of emergence of polar nanoregions in relaxor ferroelectrics, was calculated based on the $\varepsilon^{-1}(T)$ dependence (Fig. 3) to be around 100°C and was comparable to the one for SBN61 single crystals ($T_b \sim 87$°C). The values of ε in the SBN60 film were 660–860 at all the examined temperatures. In general, such values are fairly high for ferroelectric materials grown on Si substrates.

The injection-type hysteresis in MFS structures, which was seen at $U > 10$ V, is attributable to the formation of a built-in charge in the film at the interface with the substrate [9]. When a *p*-type semiconductor is used as a substrate, electrons (minority carriers) get injected from the substrate to the film as the positive voltage amplitude increases; these electrons are fixed at traps and form a negative built-in charge. Therefore, the silicon substrate surface becomes enriched with majority carriers after the removal of voltage, and the heterostructure is characterized by a capacitance up to $C_{\max}$. This sample condition is stable (C_{samp} decreased by 1.6% within the first 24 h and by 2.1% in 120 h), but the capacitance may be reduced down to $C_{\min}$ by applying a negative voltage pulse with an amplitude no lower than -10 V.

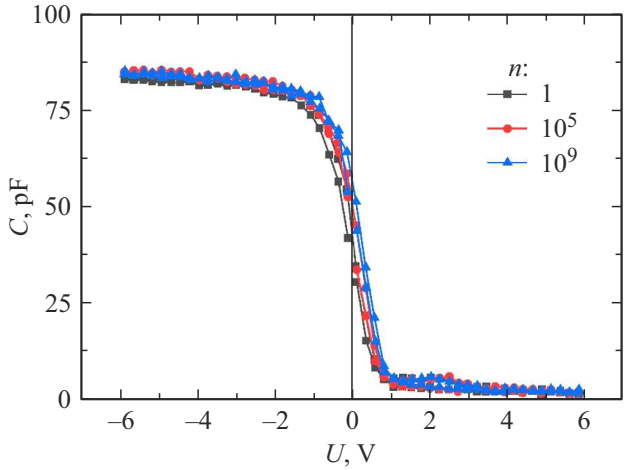

Figure 2. Room-temperature dependences $C(U)$ for the SBN60/STO/Si(001) heterostructure at $f = 10$ kHz after different numbers of switching cycles at a frequency of 10^6 Hz and $U = \pm 6$ V.

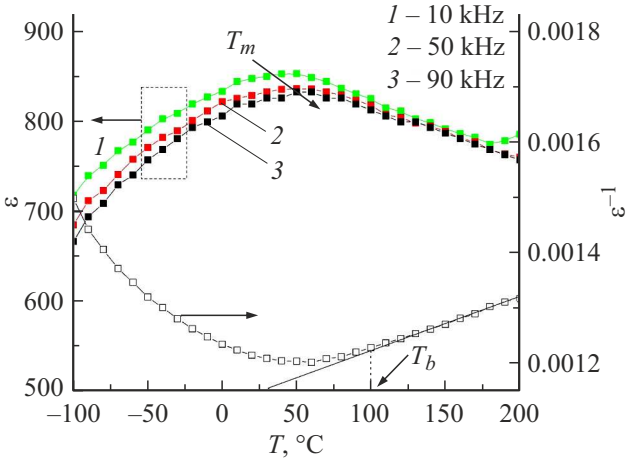

Figure 3. Dependences $\varepsilon(T)$ at various frequencies and $\varepsilon^{-1}(T, f = 90\,\mathrm{kHz})$ for the SBN60 film at T ranging from -100 to 200°C.

Thus, it was found in the examination of CVCs of SBN60/STO/Si heterostructures that, depending on the amplitude and polarity of the applied voltage, both polarization and injection hystereses may manifest themselves in such structures due to the ferroelectric field effect. It was demonstrated that these phenomena have different physical origins and the memory effects associated with them differ significantly in temporal stability. An approach providing an opportunity to study the temperature-frequency variation of ε of a ferroelectric film in an MFS structure was proposed. It allowed us to demonstrate for the first time that *c*-oriented SBN60 films grown on a semiconductor substrate are relaxor ferroelectrics with $T_b \sim 100$°C.

Funding

This study was carried out under the state assignment of the Southern Scientific Center of the Russian Academy of Sciences (the state registration number of the project is 122020100294-9).

Conflict of interest

The author declares that he has no conflict of interest.

References

[1] V.A. Gritsenko, D.R. Islamov, *Fizika dielektricheskikh plenok: mekhanizmy transporta zaryada i fizicheskie osnovy priborov pamyati* (Parallel', Novosibirsk, 2017) (in Russian).
[2] M. Dawber, K.M. Rabe, J.F. Scott, Rev. Mod. Phys., **77**, 1083 (2005). DOI: 10.1103/RevModPhys.77.1083
[3] T. Mikolajick, S. Slesazeck, H. Mulaosmanovic, M.H. Park, S. Fichtner, P.D. Lomenzo, M. Hoffmann, U. Schroeder, J. Appl. Phys., **129**, 100901 (2021). DOI: 10.1063/5.0037617
[4] V. Krayzman, A. Bosak, H.Y. Playford, B. Ravel, I. Levin, Chem. Mater., **34**, 9989 (2022). DOI: 10.1021/acs.chemmater.2c02367
[5] G.H. Olsen, U. Aschauer, N.A. Spaldin, S.M. Selbach, T. Grande, Phys. Rev. B, **93**, 180101(R) (2016). DOI: 10.1103/PhysRevB.93.180101
[6] H. Liu, B. Dkhil, J. Alloys Compd., **929**, 16731 (2022). DOI: 10.1016/j.jallcom.2022.167314
[7] S. Gupta, A. Kumar, V. Gupta, M. Tomar, Vacuum, **160**, 434 (2019). DOI: 10.1016/j.vacuum.2018.11.057
[8] S. Ivanov, E.G. Kostsov, IEEE Sensors J., **20**, 9011 (2020). DOI: 10.1109/JSEN.2020.2987633
[9] V.M. Mukhortov, Yu.I. Golovko, A.V. Pavlenko, D.V. Stryukov, S.V. Biryukov, A.P. Kovtun, S.P. Zinchenko, Phys. Solid State, **60**, 1786 (2018). DOI: 10.1134/S1063783418090202.
[10] M. Said, T.S. Velayutham, W.C. Gan, W.H.A. Majid, Ceram. Int., **41**, 7119 (2015). DOI: 10.1016/j.ceramint.2015.02.023
[11] T. Lukasiewicz, M.A. Swirkowicz, J. Dec, W. Hofman, W. Szyrski, J. Cryst. Growth, **310**, 1464 (2008). DOI: 10.1016/j.jcrysgro.2007.11.233
[12] J.J. Zhang, J. Sun, X.J. Zheng, Solid-State Electron., **53**, 170 (2009). DOI: 10.1016/j.sse.2008.10.012
[13] V.A. Gurtov, *Tverdotel'naya electronika* (PetrGU, Petrozavodsk, 2004) (in Russian).
[14] A.V. Pavlenko, D.A. Kiselev, Ya.Yu. Matyash, Phys. Solid State, **63**, 881 (2021). DOI: 10.1134/S1063783421060160.
[15] D.V. Isakov, T.R. Volk, L.I. Ivleva, Phys. Solid State, **51**, 2334 (2009). DOI: 10.1134/S1063783409110237.

Translated by D.Safin